ELSEVIER

Spherulitic morphology of electrochemically-deposited poly*para*phenylene (PPP) films

A. Mani [a], K.L.N. Phani [b],*

[a] *X-ray Diffraction Laboratory, Central Electrochemical Research Institute, Karaikudi 630 006 (TN) India*
[b] *Electrodics and Electrocatalysis Division, Central Electrochemical Research Institute, Karaikudi 630 006 (TN) India*

Abstract

Spherulitic poly*para*phenylene (PPP) films were synthesized using the microemulsion-based electrooxidation of benzene. Lower polymerization charge values yielded thin films consisting of a large population of (crystalline) spherulites whereas with higher values, (amorphous) network structures were observed. A correlation was found between the thickness-dependent morphology (and crystallinity) and luminescence characteristics. Enhancement in the crystal domain size is evident from the perfect spherulitic films. © 2001 Elsevier Science B.V. All rights reserved.

1. Introduction

Synthetic polymers crystallize when processed in melts and concentrated solutions, in the form of spherulites. Spherulites are one of the most important anisotropic structures that are useful for enhanced properties of polymers for various applications [1]. They represent a state of supermolecular order [1] and exhibit birefringence. Most polymers are randomly oriented as in *cooked spaghetti*. To improve the molecular orientation and crystal domain size in semicrystalline polymers, thermal annealing is often employed as a post-synthesis treatment [2]. However, the control of the morphology at the stage of synthesis continues to be explored in several laboratories. This is especially true in the case of conjugated polymers and achieving structurally defined material forms would be a valuable contribution to this subject area. The use of organized surfactant assemblies as templates and nucleating agents in electrochemical synthesis has great potential in control of the morphology of polymer thin films [3]. Conjugated polymers are finding niche applications in electronic, opto-electronic and electrochemical devices.

Among them, poly*para*phenylene (PPP) polymer layers are potential candidates as active layers in display devices that emit in the visible region [4–6]. Electrosynthesis of PPPs by anodic coupling of benzene or its derivatives constitutes one of the most valuable techniques for obtaining conducting PPP films of controlled thickness [7,8]. We have reported previously a microemulsion-based electrosynthetic approach to prepare thin films of PPP [9–11] by electrooxidation of benzene with a degree of polymerization of ~ 42 [9]. Herein, we report our first results on the electrochemical generation of a morphology with a large population of crystalline spherulites in the thin films of a conjugated PPP under ambient conditions and its variation by controlling the thickness of the films.

2. Experimental

The PPP films were synthesized electrochemically from a microemulsion-based electrolytic medium. Briefly, benzene monomer was solubilized in concentrated sulfuric acid (~ 18 M) using 14.8 mM sodium dodecylsulfate (SDS) (critical micelle concentration, cmc ~ 0.8 mM) or Triton X-100 (cmc ~ 0.3 mM) surfactant to yield an oil-in-water (o/w) type micro-

* Corresponding author. Fax: + 91-4565-427-779/713.
E-mail address: kanalaphani@yahoo.com (K.L.N. Phani).

emulsion. The optimum molar concentration ratio of benzene to H_2SO_4 was found to be 2:5. The films were grown on conducting indium–tin–oxide (ITO) glass (Donnelly Corp., Michigan, USA) (area ~ 1 cm^2) by cycling the potential between $+0.91$ and -0.21 V (Hg | Hg$_2$SO$_4$ | 1 M H$_2$SO$_4$ (MSE)) at 25 °C at a sweep rate (v) of 0.1 V s^{-1} using a large area platinum gauze as the counter electrode in the above microemulsion medium purged with argon gas. The ITO glass substrates were cleaned using isopropyl alcohol, Milli-Q water and a final rinse in dry acetone before use in electrolysis. The film thickness was measured in terms of the anodic charge consumed in the cyclic potentiodynamic growth pattern (mC cm^{-2}), that is, the first 12 cycles corresponded to 1.38 mC cm^{-2}, 20 cycles corresponded to 2.35 mC cm^{-2}, and 23–50 cycles to higher thickness values in the range of $2.35 < t < 5.75$ mC cm^{-2}. The films were washed with water and ethanol and dried before subjecting them to structural characterization.

X-ray diffraction patterns were recorded using a computer-controlled X-ray powder diffractometer system, JEOL JDX-8030, at a rating of 40 kV and 20 mA with Ni-filtered Cu–K$_\alpha$ radiation ($\lambda = 0.15418$ nm). The $\theta - 2\theta$ mode of scan was used to record X-ray diffraction patterns of the polymer samples. The 2θ-range was between 3 and 65° at a step scan of 0.1° (2θ) for a measuring time of 1 s for a step. The degree of crystal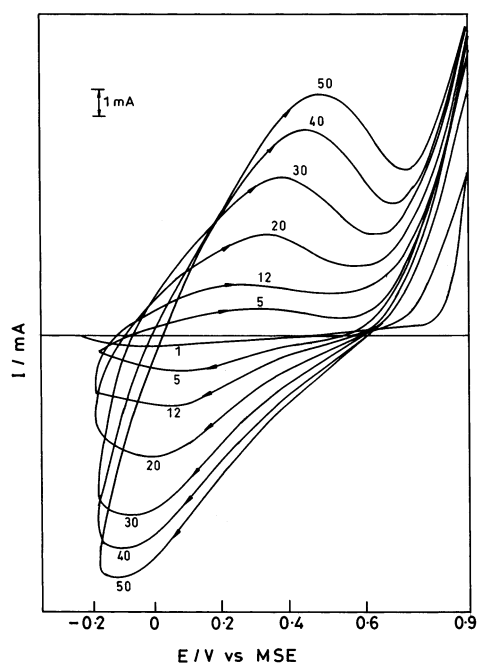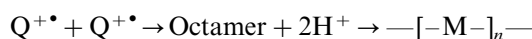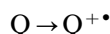linity was measured as the percentage ratio of the intensities corresponding to the crystalline volume (I_c) to that (I_a and I_c) of the whole (amorphous and crystalline) matrix. That is, degree of crystallinity, $X_{cr}/\% = [I_c/(I_a + I_c)] \times 100$.

The morphological details of the polymer film samples were recorded using a JEOL JSM-35CF scanning electron microscope at an operating voltage of up to 15 kV. The photoluminescence spectral measurements were made using a Hitachi 650-105 fluorescence spectrophotometer.

3. Results and discussion

The cyclic voltammogram (Fig. 1) for the anodic oxidation of benzene on ITO substrates in concentrated sulfuric acid containing sodium dodecylsulfate (Triton X-100) is characterized by $E_{p,a} = 0.30$ V and $E_{p,c} = 0.18$ V versus MSE. It may be noted that benzene undergoes oxidation at a rather low potential (i.e. $E_{p,a} = 0.4$ V vs. MSE) in this medium compared to many other electrolytic media [7,8]. The benzene ring (monomer, M) forms a π-complex with the proton from the sulfuric acid and its stability is lowered. This facilitates oxidation of benzene and then polymerization to give poly-*para*phenylene. It is probable that the reduction of the benzene oxidation potential which may result from a strong interaction of benzene with the proton, is due to the formation of a π-complex, more easily oxidizable than the single monomer [12,13]. It has now been demonstrated [14–16], using the oligomer approach that the dimerization reactions of the monomers and oligomers involve coupling between the electrogenerated cation radicals (radical–cation coupling) rather than the starting molecule (radical–substrate coupling). Quantitative kinetic studies on the coupling steps of oligomeric pyrroles and thiophenes which are electropolymerized in much the same way as benzene have confirmed this mechanistic approach [8,17]. The oligomerization in solution preferably occurs via consecutive 'dimerization' steps (involving a number of chemical and electrochemical (ECE) steps) leading from a dimer (D) to a tetramer (Q) and then finally to a polymer. The precipitation of the polymer occurs by coupling of oligomers in solution, according to the following mechanism:

$$M \rightarrow M^{+\bullet}$$

$$M^{+\bullet} + M^{+\bullet} \rightarrow D + 2H^+$$

$$D \rightarrow D^{+\bullet}$$

$$D^{+\bullet} + D^{+\bullet} \rightarrow Q + 2H^+$$

$$Q \rightarrow Q^{+\bullet}$$

$$Q^{+\bullet} + Q^{+\bullet} \rightarrow \text{Octamer} + 2H^+ \rightarrow -[-M-]_n-$$
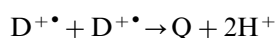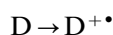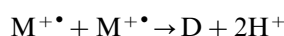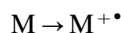

Fig. 1. Cyclic voltammogram for electro-oxidation of benzene on ITO glass substrate (~ 1 cm^2) under potentiodynamic cycling conditions in microemulsion; sweep rate: 0.1 V s^{-1} (numerals indicate cycle numbers); benzene: H$_2$SO$_4$ = 2: 5 + SDS/Triton X-100 (14.8 mM).
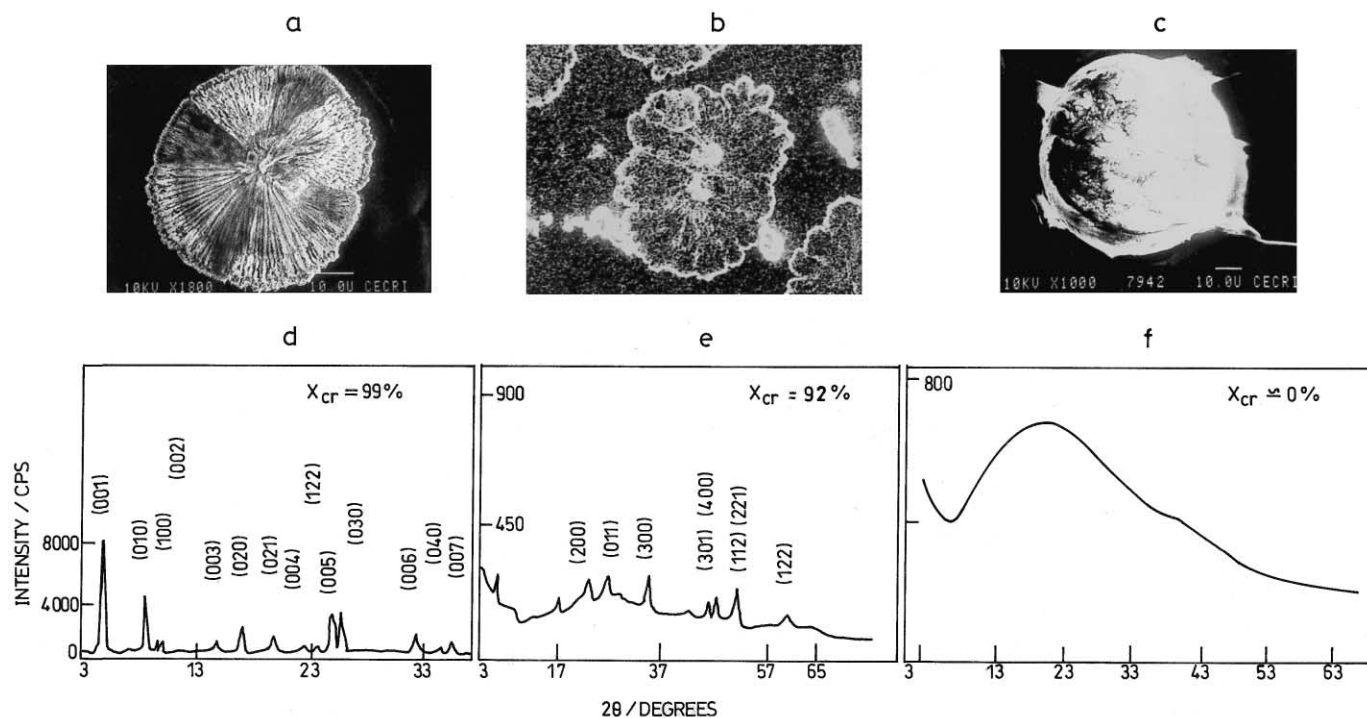
Fig. 2. (a–c) Scanning electron micrographs for PPP films with (a) perfect; (b) distorted-; (c) featureless-spherulites. (d–f) X-ray diffraction patterns corresponding to (a–c), respectively.

It is expected that there will be a greater stabilization of the radical–cations in the presence of surfactant molecules [18].

The thickness of the polymer film was increased using increasing numbers of electrochemical growth cycles. When potential cycling was carried out under voltammetric conditions, the films on the ITO substrates were found to consist of spherical particles [9–11]. At the beginning of cycling, discrete islands of polymer crystallites appeared, whereas, when the film became thicker, a loss of crystallinity was observed. Various interesting morphological textures became evident on controlling the film thickness by varying the number of electrochemical growth cycles [10,11]. Prominent among such morphologies is a large population of spherulites and variations differing in crystalline order and photoluminescence characteristics.

3.1. Spherulite morphology and luminescence characteristics

Scanning electron microscopy revealed a large population of spherulites, i.e. perfect (birefringent)-, distorted- and featureless-spherulites (Fig. 2(a–c)) synthesized under conditions specific to each type. They are also associated with different degrees of crystallinity, as shown by X-ray diffraction analysis (Fig. 2(d–f)). These anisotropic structures appear to result from a combination of the ability of the surfactant assemblies in (a) their two-dimensional organization on the electrode surface; and (b) providing nucleation and templating for the polymer growth. In case of perfect spherulitic PPP, the X-ray analaysis revealed a lamellar-type structure that supports the formation of surfactant bilayers on the electrode surface. Recently, Khimyak and Klinowski [19] reported the preparation of mesoporous silicates from synthesis mixtures containing different acid contents using Triton XN surfactants with short polyethyleneoxide (PEO) chains. In this work, Triton X-100 was found to give high quality products within a well-defined range of acid content. High quality products afforded sharper XRD peaks and narrower pore size distributions. This behaviour was attributed to the formation of high quality products due to the altered organization of the surfactant and the formation of hydrogen-bonded adducts with the PEO chains.

The perfect spherulitic PPP films having $\sim 99\%$ crystalline order (X_{cr}) show (Fig. 3) photoluminescence (λ_{em}) at 441 nm (blue emission) for an excitation wavelength (λ_{ex}) of 340 nm; distorted spherulitic films ($X_{cr} < 92\%$) show a green emission (λ_{em1}) at 516 nm along with a feeble bluish emission (λ_{em2}) at 460 nm for an excitation wavelength of (λ_{ex}) 260 nm. The featureless spherulitic films (amorphous) however, do not exhibit photoluminescence (PL), probably because the PL yield is so low that it cannot be observed. As can be seen from PL spectra (Fig. 3), the PPP thin films with perfect spherulite populations exhibit better optical

characteristics than the distorted spherulitic- and less-ordered films. This is clear evidence that an ordered organization is responsible for perfect PL emission. The perfect spherulitic PPP has well-defined atomic coordination in the local, as well as long-range molecular ordering and has distinct emission centers which exhibit a homogeneously single fluorescent band of blue emission. With slightly less ordered distorted spherulitic PPP, perturbation occurs in the atomic coordination symmetry giving rise to multiple emission centers to exhibit two additional emission peaks of green and a satellite peak, in addition to the less-intense blue emission. In the third case where long-range ordering is completely absent and short-range order alone exists, only the non-radiative path of localized phonons and their absorption might occur so that optical emission is completely absent.

In the case of perfect spherulites, there exists a definite crystallographic basis of three mutually orthogonal axes. The spherulitic fast growth direction along the a-axis is parallel to the crystallographic a-axis and grows radially outward from the nucleating center of the spherulite; and this results in a specific arrangement of the crystalline order (X_{cr}). The wider the radial fibril along the crystallographic b-axis, the higher will be the X_{cr} (the longer the coherence or conjugation length, the higher is the molar mass). Each radial fibril is essentially a single crystal [1]. As the spherulite forms, the axis of the crystal is aligned parallel to the radial fibril axis. Thus, all the radial fibrils in the spherulite have a specific alignment with respect to the other crystals within the spherulite. More closely, in PPP radial fibrils, regularly folded chain lamellae are aligned with the a-axis parallel to the radial fibril direction. These crystals seem to be connected (both along and between

the radial fibrils) through tie molecules that enter the crystallization process. Thus, a perfect spherulite with wider radial fibrils possesses a higher crystalline order, $X_{cr} = 99\%$ and distorted spherulites with 'discontinuous' random fibrils exhibit $X_{cr} = 92\%$ only. The formation of spherulites with radial fibrils is clearly a manifestation of enhanced crystal domain size and the observed crystal domain size is 1.5 μm × 25 μm. In addition, the repeat chain length in the unit cell region is computed to be 1.766 nm which is more than twice the value reported earlier [20] indicating a higher conjugation length of the PPP polymer. The molar mass is calculated to be larger than 1×10^6 amu. The molecular orientation is found to be along the crystallographic c-direction ([001] propagation). This structural order is facilitated since 2D organization is possible with the surfactant assemblies. The surfactant bilayers formed on the electrode surface solubilize the monomer at the electrochemical interface where the latter undergoes oxidative polymerization. Such an organizing ability of the surfactant bilayers was demonstrated in the case of polymers like polypyrrole [21] (columnar microstructures observed by SEM and AFM) and substituted polythiophenes [18]. The surfactant assemblies on the electrode surface can also act as nucleating agents for the ordered polymer growth. Strong electrostatic interactions occurring between the oxidized monomer species and dodecylsulfate anions can lead to the formation of a strongly bonded complex between these entities. Furthermore, benzene electropolymerization in a microemulsion (sodium dodecylsulfate as the surfactant) produces well-organized, adherent films on the ITO electrode. Previously, Lal et al. [22] reported polymerization in reverse micellar nano-reactors to obtain processable poly(p-phenylenevinylene) with a controlled conjugation length.
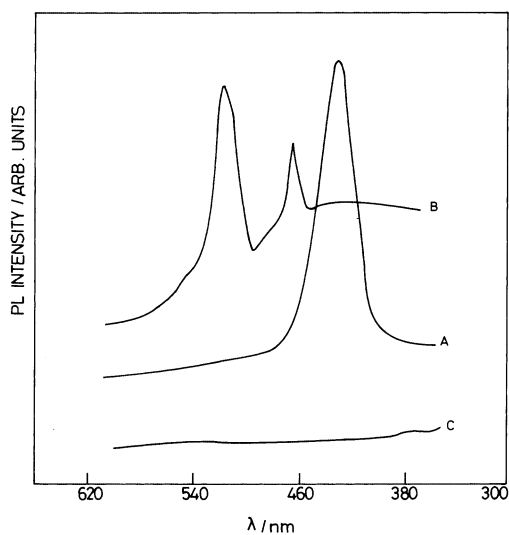
3.2. Morphological characteristics versus electrochemical growth cycles

The morphological characteristics along with crystalline order of PPP thin films with electrochemical growth cycles have been studied and the results are summarized in Table 1. The degree of crystallinity (X_{cr}) decreases with increasing growth cycles, particularly well beyond 2.65 mC cm^{-2}. Initially, X_{cr} is measured to be 99% for a perfect spherulite morphology (of film thickness = 1.38 mC cm^{-2}) which becomes distorted at a thickness of 2.65 mC cm^{-2} at $X_{cr} = 92\%$ and then drastically reduced to $X_{cr} = 0\%$ at thickness ≥ 4.46 mC cm^{-2} giving rise to random network microstructures. At an intermediate stage of thickness of 3.45 mC cm^{-2}, a mixed morphology of a random network with globules is seen, for which $X_{cr} < 30\%$ (partially crystalline, the diffraction pattern not shown). Independently of the surfactant, SDS or Triton X-100 and growth cycles

Fig. 3. Photoluminescence spectra corresponding to (a) perfect-; (b) distorted-; (c) featureless-spherulitic PPP films.

Table 1
Morphological characteristics and crystalline order of PPP thin films vs. anodic charge

Anodic charge [a]/mC cm^{-2}	Degree of crystaliinity/%	Morphology	
		Structure	SEM, Fig.
1.38	99	Perfect spheruiite	
		Wider radical fibrils	1(a)
1.76	97	Perfect spherulite	
		Thinner radical fibrils	3(a)
2.08	95	Perfect spherulite	
		Still thinner radical fibrils	3(b)
2.65	92	Distorted spheruiite	
		Randomfibrils	1(d)
3.45	<30	Mixed: random network + giobular	3(c)
4.46	0	Random network (fibrils)	3(d)
5.75 (SDS)	0	Random network (fibrils)	3(e)
5.75 (Triton X-100)	0	Random network (fibrils)	3(f)

[a] Films grown in microemulsion containing SDS (14.8 mM) surfactant except for Fig. 3(f) which corresponds to Triton-X-100 (14.8 mM).

≥ 4.46 mC cm^{-2}, different features of random network (fibrous) structures are noticed, indicating completely disordered (non-crystalline) characteristics. The systematic changes in morphology with the electrochemical growth pattern are given in Figs. 2(a), 4(a), 4(b), 2(b), 4(c), 4(d), 4(e) and 4(f) corresponding to thickness values of 1.38, 1.76, 2.08, 2.65, 3.45, 4.46, 5.75 (SDS) and 5.75 (Triton X-100) mC cm^{-2}, respectively.

In the conjugated polymers, the electron- and ion-transport behaviour strongly depend on the solid state structural aspects, particularly crystalline order and morphology in thin films. For example, the electronic or electrical conductivity is largely controlled by inter-chain transport that depends mainly on the alignment of the macromolecular chains in the film matrix; also the extent of doping/de-doping depends on the polymer morphology [23]. Hence, the reported morphology and crystalline order characteristics have a strong influence on the structure-sensitive properties like electronic conductivity. Komaba et al. [24], in their study on PPP obtained by electrooxidation of biphenyl in acetonitrile medium, observed a decrease in the intensity of EL emission with increasing polymerization charge, i.e. an electrochemical depth profile. Their results are comparable to the present observation of the effect of electrochemical growth cycles, i.e. thickness on the PL characteristics. There have been similar reports on the thickness (and morphology)-dependent structural characteristics in the case of electrosynthesized polyaniline films [25]; for a thickness of 10 mC cm^{-2}, a globular (crystalline) morphology is seen while a thicker (60 mC cm^{-2}) deposit develops a fibrous (amorphous) structure. Increasing thickness renders the conjugated polymer more disordered. Also, in the case of 'surface grown' polypyrrole [26], a conjugation length longer than that of the conventional versions of this polymer was observed due to predominant α–α' linkages of

monomers (with only a few α–β monomer linkages which are undesirable for extended conjugation). This is attributed to the adsorption process causing two pyrrole rings to be coplanar during bond formation in the surface adsorbed material. These reports [27,28] have also shown that the chain linearity-inducing influence of the surface is diminished as the film thickens. One another factor that may be responsible for this disorder at higher thickness values is the convective forces operating at the electrode surface due to the depletion of the monomer at the electrode surface as the electrolysis proceeds to form thick films. Thus, the crystalline (long range) ordering of the macromolecules corresponding to 'real' thin films is lost to become less crystalline or amorphous, indicating setting-in of bulk characteristics due to possible complex molecular defects.

4. Conclusions

We have reported in this paper, an electrochemical method to obtain a variety of highly ordered spherulitic morphologies in conjugated poly*para*phenylene polymer and a correlation of morphology and crystalline order (vs. electrochemical growth cycles) to the luminescence characteristics. Most importantly, this work proves that spherulites are not confined only to polymers processed in melts and concentrated solutions, but can also be obtained by electrodeposition. The role of the surfactant in electrosynthesis is also evident from the variety of textures possible under the conditions employed in this study. This study shows that the film morphology depends significantly on the thickness and in turn influences the properties of the film. An obvious next step in this work is to follow the nucleation process, which is in the first stages of film growth in the
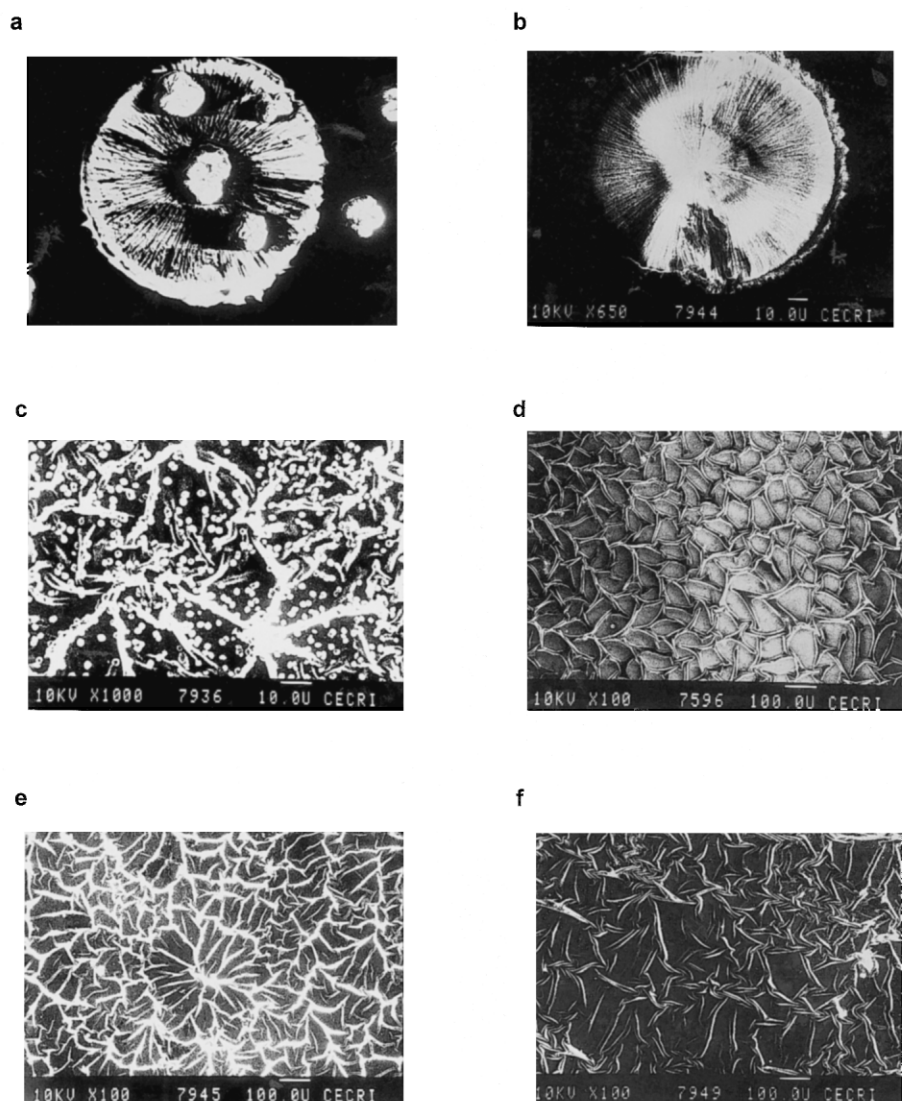
Fig. 4. SEM morphology of PPP thin films for different electrochemical growth cycles: 1.76; (b) 2.08; (c) 3.45; (d) 4.46; (e) 5.75 (SDS) and (f) 5.73 (Triton X-100) mC cm^{-2}.

presence of surfactants. Our current work addresses the issues concerning nucleation/growth mechanisms based on the theoretical concepts that have been developed for the electrocrystallization of metals [29] and later applied to conducting polymers [18,30,31]. The mechanism of the action of surfactants in the electrodeposition of conducting polymers should be of immense interest and can be followed using electrochemical transient techniques. We are currently applying such techniques to study their role in the evolution of polymer microstructures (morphology vs. electrochemical potential programmes).

In the context of materials for opto-electronic devices, the applicability of this method to polymer materials remains to be seen. The candidate polymer systems we propose to employ are the processable PPP-ladder polymers of the type being explored by Leising and coworkers [32,33]. One of the benefits of spherulite morphology is that they offer the right starting materials for stretch-orientation; even at low stretching levels, a high degree of orientation is expected [1]. Work by Son et al. [34] indicates that the PL efficiency can be increased in a polymer by separating the polymer chains. In our opinion, it becomes easier to achieve this condition by stretching the spherulitic films. Polarized emission [35] is also possible with such stretch-oriented films.

Acknowledgements

References

[1] R.J. Samuels, Structured Polymer Properties, Wiley, New York, 1974.

[2] S. Sasaki, T. Yamamoto, T. Kanbara, A. Morita, T. Yamamoto, J. Polym. Sci. Part B Polym. Phys. 30 (1992) 293.

[3] Report of the Committee on Polymer Science and Engineering USA, Polymer Science and Engineering—Shifting Research Frontiers, National Academy Press, Washington, DC, 1994.

[4] G. Grem, G. Ledtzky, B. Ullrich, G. Leising, Adv. Mater. 4 (1992) 36.

[5] W. Graupner, G. Leising, G. Lanzani, M. Nisoli, S. De Silvestri, U. Scherf, Chem. Phys. Lett. 246 (1995) 95.

[6] C. Paar, S. Stampfl, S. Tasch, H. Kreimaier, G. Leising, H. Vestweber, J. Pommerehne, H. Bassler, U. Scherf, Solid State Commun. 96 (1995) 167.

[7] L.M. Goldenberg, P.C. Lacaze, Synth. Metals 58 (1993) 271.

[8] P.C. Lacaze, S. Aeiyach, J.C. Lacroix, in: H.S. Nalwa (Ed.), Handbook of Organic Conductive Molecules and Polymers. Conductive Polymers: Synthesis and Electrical Properties, vol. 2, Wiley, New York, 1997, pp. 205–270 Ch. 6.

[9] K.L.N. Phani, S. Pitchumani, S. Ravichandran, S. Tamil Selvan, S. Bharathey, J. Chem. Soc. Chem. Commun. (1993) 179.

[10] S. Tamil Selvan, A. Mani, S. Pitchumani, K.L.N. Phani, J. Electroanal. Chem. 384 (1995) 183.

[11] A. Mani, S. Tamil Selvan, K.L.N. Phani, J. Solid State Electrochem. 2 (1998) 242.

[12] L.M. Goldenberg, S. Aeiyach, P.C. Lacaze, J. Electroanal. Chem. 327 (1992) 173.

[13] L.M. Goldenberg, S. Aeiyach, P.C. Lacaze, Synth. Metals 51 (1992) 343.

[14] A. Smie, A. Synowczyk, J. Heinze, R. Alle, P. Tschuncky, G. Götz, P. Bäuerle, J. Electroanal. Chem. 452 (1998) 87.

[15] L. Guyard, P. Hapiot, P. Neta, J. Phys. Chem. B 101 (1997) 5698.

[16] J. Heinze, in: H. Lund, O. Hammerich (Eds.), Organic Electrochemistry, 4th ed., Marcel Dekker, New York, 2000, p. 1309.

[17] P. Audebert, J.-M. Catel, G. Le Coustumer, V. Duchenet, P. Hapiot, J. Phys. Chem. B 102 (1998) 8661.

[18] N. Sakmeche, S. Aeiyach, J.-J. Aaron, M. Jouini, J.C. Lacroix, P.-C. Lacaze, Langmuir 15 (1999) 2566.

[19] Y.Z. Khimyak, J. Klinowski, J. Mater. Chem. 8 (2000) 1847.

[20] Z. Mo, K.B. Lee, Y.B. Moon, M. Kobayashi, A.J. Heeger, F. Wudl, Macromolecules 18 (1985) 1972.

[21] K. Naoi, Y. Oura, M. Maeda, S. Nakamura, J. Electrochem. Soc. 142 (1995) 417.

[22] M. Lal, N.D. Kumar, M.P. Joshi, P.N. Prasad, Chem. Mater. 10 (1998) 1065.

[23] K. Miyashita, M. Kaneko, J. Electroanal. Chem. 403 (1996) 53.

[24] S. Komaba, A. Amano, T. Osaka, J. Electroanal. Chem. 430 (1997) 97.

[25] C.M. Randolph, J. Desilvesto, J. Electroanal. Chem. 262 (1989) 289.

[26] H.S.O. Chen, L.M. Gan, H. Chi, C.S. The, J. Electroanal. Chem. 379 (1994) 293.

[27] Z. Cai, C.R. Martin, J. Electroanal. Chem. 300 (1991) 35.

[28] R.V. Gregory, W.C. Kimbiell, H.H. Kaun, Synth. Metals 28 (1989) 823.

[29] M. Fleischmann, H.R. Thirsk, in: P. Delahay (Ed.), Advances in Electrochemistry and Electrochemical Engineering, vol. 3, Wiley Interscience, New York, 1963, p. 63.

[30] A.R. Hillman, E.F. Mallen, J. Electroanal. Chem. 220 (1987) 35.

[31] A.J. Downard, D. Pletcher, J. Electroanal. Chem. 206 (1986) 139.

[32] S. Tasch, A. Niko, G. Leising, U. Scherf, Phys. Rev. B Condens. Matter 56 (1997) 4479.

[33] S. Tasch, A. Niko, G. Leising, U. Scherf, Appl. Phys. Lett. 71 (1997) 2883.

[34] S. Son, A. Dodabalapur, A.J. Lovinger, M.E. Galvin, Science 269 (1995) 376.

[35] P. Dyreklev, M. Berggren, O. Inganäs, M.R. Andersson, O. Wennerström, T. Hjertberg, Adv. Mater. 7 (1995) 43.